Trans. JSASS Aerospace Tech. Japan
Vol. 17, No. 4, pp. 512-518, 2019
DOI: 10.2322/tastj.17.512

Flight Control Parameter Design for Mars Airplane Balloon Experiment-1 (MABE-1) Using Evolutionary Computation

By Koji FUJITA,[1] Hiroshi TOKUTAKE,[2] Hiroki NAGAI,[3] and Akira OYAMA[1]

[1] *Institute of Space and Astronautical Science, JAXA, Sagamihara, Japan*
[2] *Kanazawa University, Kanazawa, Japan*
[3] *Institute of Fluid Science, Tohoku University, Sendai, Japan*

(Received June 23rd, 2017)

Airplanes are paid attention as a new platform for Mars exploration. A high-altitude flight test using balloon was conducted in June 2016 by Japanese working group for Mars exploration aircraft. This paper reports a method of control gain tuning for the flight test using evolutionary computation approach. This method can find optimal robust control gains efficiently and automatically. The combination of the control gains are evaluated by the simulations of a finite number of the dispersion conditions defined by the sensitivity analysis. A summary of a flight test, a control law, an optimization method, a flight simulation method, an evaluation function setting, and an optimization result are described.

Key Words: Mars Airplane, High Altitude Flight Test, Control, Evolutionary Computation, Flight Dynamics

Nomenclature

A : sensitivity coefficient
C_{lp} : derivative of rolling moment with respect to roll rate
C_{lr} : derivative of rolling moment with respect to yaw rate
C_M : pitching moment coefficient
C_q : correction factor for dynamic pressure
da : aileron deflection
E : evaluation function
g : gravity
h : height
$KaIp$: roll-rate-integral gain for aileron
Kap : roll-rate-proportional gain for aileron
$KrIr$: yaw-rate-integral gain for rudder
Krr : yaw-rate-proportional gain for rudder
N : number of simulation condition
P : roll rate
PI : proportional-integral (control)
p : penalty
q : dynamic pressure
R : yaw rate
R_{Earth} : radius of the Earth
T : atmospheric temperature
W : weight coefficient
Δt : time step
θ : pitch angle
ρ : atmospheric density
ϕ : roll angle
ϕ_{diff} : difference of horizontal component of wing upper surface direction and the desired heading in last 2 seconds of roll phase
ψ : heading (i.e. direction of airplane X-axis in horizontal plane)
ψ_{up} : upper surface direction of airplane
ψ_{diff} : difference of heading and the desired heading in last 4 seconds of pull-up phase

Subscripts
0 : initial
c : desired value
nom : nominal
$Pull$: pull-up phase
$Roll$: roll phase
s : standard

1. Introduction

Airplane for Mars exploration (Mars airplane) is a new Mars observation platform that enables wide-range observation from low altitude. Since 2010, the working group for Mars exploration aircraft has been working on concept design and fundamental researches of Mars airplane.[1] A high-altitude flight test named "Mars Airplane Balloon Experiment-1 (MABE-1)" was conducted to measure the aerodynamic performance of a Mars airplane.[2,3] Even on Earth, the flight condition at the altitude of 36 km is almost same as the condition on Martian surface except the difference of the gravity.

The control system for the MABE-1 required various considerations. The flight area was restricted to secure the safety of civil flights. Because the mass of the airplane was severely restricted, the stiffness of the structure was relatively low and the equipped sensors were limited in number and low in accuracy. The uncertainties were large because it was first

J-STAGE Advance published date: January 31st, 2019

flight of this airplane. The airplane needed roll and pull-up maneuvers before gliding flight because the airplane was dropped from the airplane as shown in next chapter. Usually, the accelerometers and the rate gyros are calibrated just before the flight in quiescent state. However, the airplane for the MABE-1 could not calibrate just before the flight because the airplane was hanged and swinging under the balloon. The sensors were anticipated to offset due to the temperature change from the ground to the high altitude.

The airplane for this flight test was controlled by Proportional-Integral (PI) controller. Usually, a tuning of the control parameters is performed by trial and error. This procedure takes much time and efforts. In addition, another problem of the flight control was the uncertainties of the flight simulation such as the flight environment, the initial conditions, the sensor errors, and the modelling errors. The determined control parameters must ensure safe flight under such uncertainties.

To solve the parameter tuning problem, an evolutionary computation technique has been applied by handling the control parameters as design parameters of the optimization problem.[4] The control parameters can be tuned automatically and efficiently by using the evolutionary computation techniques. This technique also has been applied for aerospace problems. Krishnakumar et al. used a genetic algorithm technique to design a lateral autopilot and a windshear controller. They revealed that a variety of aerospace control system optimization problems can be addressed using genetic algorithms with no special problem-dependent modifications.[5] As shown above, the parameter tuning problem can be solved thorough optimization technique.

There are two different approach to obtain a robust controller. One is an analytical method and another is a statistical method.

As examples of the analytical method, Ghazi et al. proposed a robust controller design method using a linear quadratic regulator theory, a guardian map theory, and a genetic algorithm.[6] Avanzini et al. used an evolutionary algorithm in the framework of H_∞ control theory for an unstable aircraft.[7] However, these analytical methods were not optimal for the controller design for MABE-1 because the estimated uncertainties in MABE-1 were quite large in both number and standard deviation. When the uncertainties are too various and large, such analytical method usually cannot find the solution. Even if the solution is found, the obtained solution is usually too conservative value. Therefore classical PID theory was considered. The differential term was not able to use for MABE-1 because the noise was also large. Therefore, PI controller was selected. In addition, in the case of a preflight evaluation of the control system such as this paper, the value of each standard deviation for controller analysis was clearly defined in advance. Therefore, the controller should be directly optimized for those defined uncertainties.

The statistical method evaluates the controller by statistic values such as a rate of the constraint violation. Motoda et al. applied one of the stochastic parameter optimization methods to solve the flight controller design for the airplane that has uncertainties.[8] They evaluated the controller through the Monte-Carlo simulation and optimized using the combination of the simulated annealing method and the downhill-simplex method. However, this method requires a lot of computation resources to perform the Monte-Carlo simulation for each evaluation.

In this paper, a low-cost and automatic parameter tuning method considering uncertainty is proposed. Each individual (i.e. the combination of the control parameters) was directly evaluated through simulations with uncertainties. Here, the evaluation was performed by not the Monte-Carlo simulations but the simulations of a finite number of the dispersion conditions defined by the sensitivity analysis to reduce the calculation cost. The proposed method is able to deal with multi-parameter problem such as the controller design for MABE-1 because the calculation cost is relatively low. Also, the proposed method is able to optimize the design parameters even if the evaluation function is multimodal, because the proposed method uses the evolutionary computation technique. This method can be used for optimization of any system that has defined uncertainties, such as a controller design of a pre-flight airplane. This paper presents the overview of the control law, the optimization problem establishment, the optimization methodology, and the results of the PI controller design for MABE-1.

2. Overview of the MABE-1

Figure 1 and Table 1 show the outline drawing and the principal dimensions of the airplane for MABE-1. Because this test was the first trial, the objective of the test was set to perform basic maneuvers and to obtain the aerodynamic characteristics. Therefore, this airplane had no propulsion system. The control surfaces of this airplane were the ailerons, the rudders, and the elevator. Figures 2 and 3 show the flight test sequence and the time series data at nominal flight. The flight test was conducted over the sea for the safety reason. First, the airplane was ascended to 36 km height by the balloon. Here, the airplane had been hanged inside the gondola to be protected from strong sunlight and cold atmosphere. After the health check, the airplane was released from the gondola and started dropping with aiming its nose downwards. Then the airplane performed the roll and pull-up maneuvers. The desired heading, i.e. desired direction of airplane X-axis in horizontal plane, was set to 127 degrees (clockwise from the north), i.e. the direction from land to sea, for the safety. The airplane was controlled to pull-up toward this direction. Available sensors were the 3-axial rate gyro and the dynamic pressure sensor on the airplane, and the 2-axial magnetic compass on the gondola. Note that an air data sensor (ADS) was equipped but not used for the control because this time was a first trial of the usage of the ADS at high altitude environment and therefore the reliability was unknown.

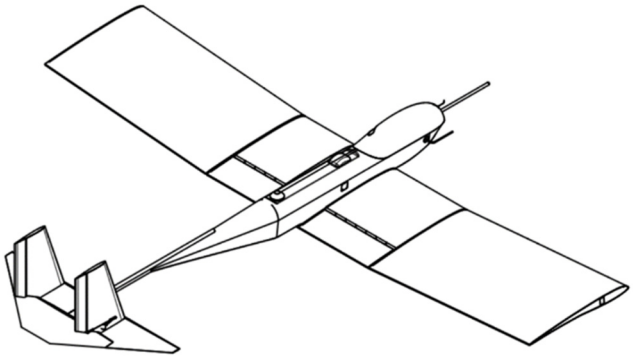

Fig. 1. Outline drawing of airplane for MABE-1.

Table 1. Principal dimensions of airplane for MABE-1.

Items	*Values*	*Units*
Airplane length (w/o ADS)	2.00	m
Wing span	2.40	m
Chord length	0.49	m
Height (w/o attitude sensor)	0.43	m

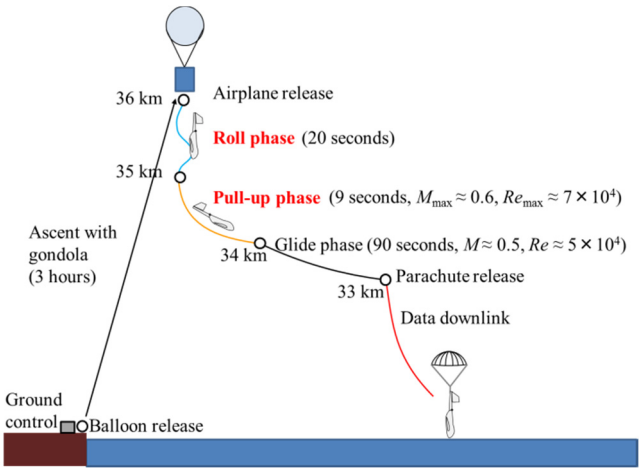

Fig. 2. Flight test sequence.

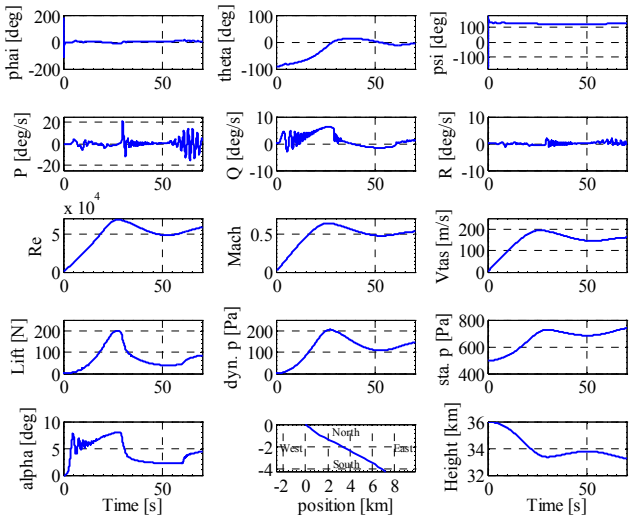

Fig. 3. Time series data at nominal flight (0-70 seconds).

3. Control Law

This paper deals with the lateral and directional controls from the airplane release to the end of the pull-up maneuver. The requirement for this control was that the absolute difference between the desired heading and the airplane heading at the end of the pull-up phase was within 60 degrees. This control has two phases: a roll phase and a pull-up phase.

In the roll phase, the airplane was controlled to aim horizontal component of the wing upper surface direction to the desired heading for the pull-up maneuver. Only the ailerons were used in this phase. The desired roll rate P_c was obtained by the following equation:

$$P_c = A\,\mathrm{ShiftAngle}(\psi_c - \psi_{up}) \tag{1}$$

where

$$\psi_{up} = \psi_0 + \sum P\Delta t \tag{2}$$

Here, a function "ShiftAngle(x)" converts an angle x [rad] into $-\pi$ to π (e.g. ShiftAngle(1.5π) = -0.5π). The upper surface direction was estimated by the integral of the yaw rate. Usually, the integral of the output of the rate gyro is not accurate. However, the integral is acceptable for this case because the integral time is short. The ailerons deflection angle da was controlled to follow the roll rate P to the desired roll rate P_c by the following proportional-integral controller:

$$da_{Rollnom} = Kap_{Roll}(P_c - P) + KaIp_{Roll}\sum(P_c - P)\Delta t \tag{3}$$

Note that, however, all control surfaces were fixed for the first 2 seconds to prevent from contacting with the gondola.

In the pull-up phase, both the ailerons and the rudders were used for a stabilization control. Note that any other controls such as a heading control or a roll angle control were performed. Both the desired roll and yaw rates were set to 0. The ailerons deflection angle da and the rudders deflection angle dr were controlled to follow the roll and yaw rates P, R to the desired roll and yaw rates P_c, R_c respectively by the following proportional-integral controllers:

$$da_{Pullnom} = Kap_{Pull}(P_c - P) + KaIp_{Pull}\sum(P_c - P)\Delta t \tag{4}$$

$$dr_{Pullnom} = Krr_{Pull}(R_c - R) + KrIr_{Pull}\sum(R_c - R)\Delta t \tag{5}$$

In this flight profile, the dynamic pressure q varies widely from zero to several hundred Pa. The effectiveness of the control surface is depends on the dynamic pressure. Therefore, the correction factor for the dynamic pressure C_q was multiplied to the nominal defection angle of the control surface.

$$C_q = q_s / \max(q, 50) \tag{6}$$

Here, the standard dynamic pressure q_s was set to 120 Pa based on the nominal dynamic pressure in gliding phase. If the dynamic pressure was less than 50 Pa, the denominator of Eq. (6) was replaced to 50 Pa to avoid divergence. The threshold

pressure 50 Pa was determined as a sufficiently low and well observable value using ADS.

The bandpass filter was used to the output of the rate gyro. Its passband was set form 0.001 Hz to 6 Hz based on the prior examination. If the deflection angle reached its mechanical limit, the integral was paused. As a longitudinal control, the elevator deflection angle was fixed to -15 degrees based on trim data of the aerodynamic model.

4. Optimization Method

Table 2 shows the design variables and its search range of the optimization. The optimization process searched the combination of these design variables that bring better headings and stable flight performance under the various off-nominal conditions.

MATLAB's Genetic Algorithm Toolbox, especially *ga* function, was employed for the current work. This function is based on the genetic algorithm. The population size was set to 50 based on prior examination. The optimization was terminated when the dispersion of the evaluation functions in the generation reached to sufficiently small value. Initial population was generated randomly. The percentage of the elites was set to 5%. The method for parent selection was the stochastic universal sampling. The ratio between crossover and mutation was 4:1. An optimal set of the control gains can be obtained through minimizing the evaluation function.

The optimization was performed for each phase. First, the proportional and integral gains for the ailerons were optimized by the simulation from the airplane release to the end of the roll phase. Then, the proportional and integral gains for the ailerons and the rudders were optimized by the simulation from the end of the roll phase to the end of the pull-up phase. Here, an initial condition for the pull-up phase was obtained as a result of the simulation from the release to the end of the roll phase with optimized gains.

The evaluation function was defined considering the ability to pull-up toward the desired heading under a finite number of the dispersion conditions selected by the sensitivity analysis to reduce the calculation cost. By this method, the robust control gain settings under the various off-nominal conditions can be achieved. As the dispersion conditions, 35 principal conditions was selected based on the sensitivity analysis. The 12 basic dispersions are shown in Table 3. Here, the amount of the effects of these 12 basic dispersions accounted for over 70% of the total amount of change in sensitivity analysis. In particular, the influence of the atmospheric density was large. Therefore, in each simulation, only one of the basic 12 dispersions was fluctuated under the positive, zero, or negative density fluctuation condition. The evaluation value of each design individual was calculated as the sum of the evaluation values of 36 simulations (i.e. 35 dispersion conditions plus 1 nominal condition). Because the 36 dispersion conditions included the conditions that two high sensitivity parameters simultaneously took bad values, the 36 dispersion conditions were eligible for robustness evaluation.

The evaluation function for the roll phase was as follows:

Table 2. Design variables and search range of optimization.

Design variables		*Range*
$Kap_{Roll\ nom}$	Proportional gain of ailerons in roll phase	0 ~ 3
$KaIp_{Roll\ nom}$	Integral gain of ailerons in roll phase	0 ~ 2
$Kap_{Pull\ nom}$	Proportional gain of ailerons in pull phase	0 ~ 3
$KaIp_{Pull\ nom}$	Integral gain of ailerons in pull phase	0 ~ 2
$Krr_{Pull\ nom}$	Proportional gain of rudders in pull phase	-3 ~ 0
$KrIr_{Pull\ nom}$	Integral gain of rudders in pull phase	-2 ~ 0

Table 3. 12 basic dispersions.

Names	*Dispersions*	*Units*	*Rationales*
C_M modelling error	0.0245	-	Wind tunnel test
Incident angle error of aileron	2	deg	Alignment measurement
Aeroelastic deformation dispersion of dihedral	10	%	Wind tunnel test
Aeroelastic deformation dispersion of twist	10	%	Wind tunnel test
Incident angle of vertical tail	0.3	deg	Alignment measurement
C_{lp} modelling error	50	%	DATCOM
C_{lr} modelling error	50	%	DATCOM
Spanwise center of gravity position error	3	mm	Alignment measurement
Alignment of twist	0.42	deg	Alignment measurement
Atmospheric pressure change	134	Pa	Height, Weather
Atmospheric temperature change	10	degC	Height, Weather
Atmospheric density change	0.0017	kg/m^3	Height, Weather

$$E_{Roll} = \sum_{1}^{N}\left(W_1 \max(|\phi_{diff}|) + W_2 \sum |P| + W_3 p\right) \tag{7}$$

In the first term, ϕ_{diff} represents the difference of the horizontal component of the upper surface direction of the airplane and the desired heading in last 2 seconds of the roll phase, as shown in Fig. 4. The design individuals that show better roll control performance can be found by evaluating the maximum value of the absolute value (i.e. the worst value) of ϕ_{diff}. The second term represents a time integral of the absolute value of the roll rate to find the solution which performs minimum roll motion. The third term represents the penalty function that becomes non-zero only if the simulation failed before the end of the phase. In this study, the penalty function was set to an uncalculated time length (i.e. the time length from the failed time to the end of the phase). As shown above, several evaluation criteria were integrated into the single evaluation function by the weighted sum to save calculation cost. The weight coefficients W_1, W_2, and W_3 were set to 10^{-1}, 10^{-5}, and 10^3, respectively. These values were determined based on a priority of each term and a magnitude of each term without weight. Here, the order of priority was the third term, the first term, the second term in descending order.

The evaluation function for the pull-up phase was as follows:

$$E_{Pull} = \sum_{1}^{N}\left(W_4 \max(|\psi_{diff}|) + W_5 \min(|\theta|) + W_6 \max(|\phi|) + W_7 p\right) \tag{8}$$

In the first term, ψ_{diff} represents the difference of the

heading of the airplane and the desired heading in last 4 seconds of the pull-up phase, as shown in Fig. 5. The design individuals that show better heading can be found by evaluating the maximum value of the absolute value (i.e. the worst value) of ψ_{diff}. The second term represents the minimum value of the absolute value of the pitch angle in last 4 seconds of the pull-up phase. The design individuals that success pull-up can be found by this term. The third term represents maximum value of the absolute value of the roll angle in last 4 seconds of the pull-up phase. The fourth term was the penalty function. It is similar to that in roll phase. The weight coefficients W_4, W_5, W_6, and W_7 were set to 5, 1/15, 0.1, and 10^3, respectively. Here, the order of priority was the fourth term, the first term, the second term, the third term in descending order.

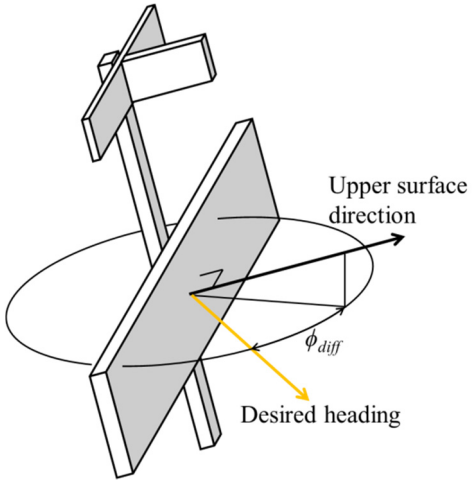

Fig. 4. Definition of ϕ_{diff}.

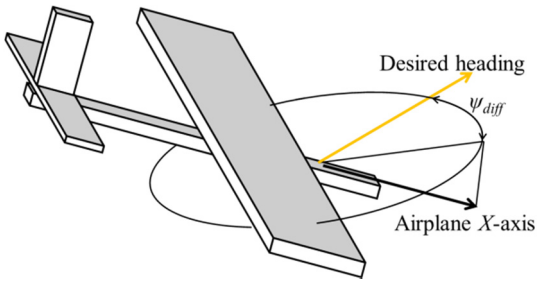

Fig. 5. Definition of ψ_{diff}.

5. Flight Simulation Method

The principal dimensions of the airplane for MABE-1 is shown in Table 1. The inertial matrix was obtained by the 3D-CAD drawings. The aerodynamic model was established based on the wind tunnel testing result of the scale model.[9] The control period was 0.05 second. The time step of the simulation was set to 0.005 second. The solver was 4th order Runge-Kutta method. The sensor output that were used for control were calculated from the true values using sensor model. Table 4 shows the nominal release condition. The airplane was released from the gondola with aiming its nose downwards.

Table 4. Nominal release condition.

Variables	*Values*	*Units*
Height	36,000	m
3-axial translational velocity	0	m/s
3-axial angular rate	0	deg/s
Roll angle	0	deg
Pitch angle	-90	deg
Yaw angle	ψ_c (=127)	deg

The gravity acceleration g was calculated as follows:

$$g = g_s\left(\frac{R_{Earth}}{R_{Earth}+h}\right)^2 \tag{9}$$

where the gravity acceleration at the ground g_s and the radius of the Earth R_{Earth} were 9.80665 m/s^2 and 6,378,100 m, respectively. The viscosity coefficient was obtained using the Sutherland's law. The atmospheric density ρ and temperature T were calculated as a function of the height h.

$$\rho[\mathrm{kg/m^3}] = 1.97576\exp(-0.00015575\,h[\mathrm{m}]) \tag{10}$$

$$T[\mathrm{degC}] = 0.002768\,h[\mathrm{m}] - 133.534353 \tag{11}$$

6. Results and Discussion

Figure 6 shows the transition of the evaluation function in roll phase optimization. It indicates that the optimization was sufficiently converged. Figure 7 shows the distribution of the evaluation value on the design space. The optimal combination of the aileron gains was obtained as [$Kap_{Roll\ nom}$, $KaIp_{Roll\ nom}$] = [0.0861, 0.0822].

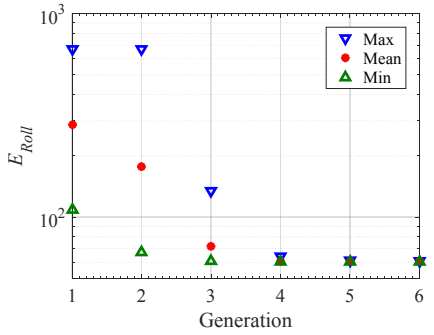

Fig. 6. Transition of evaluation function in roll phase optimization.

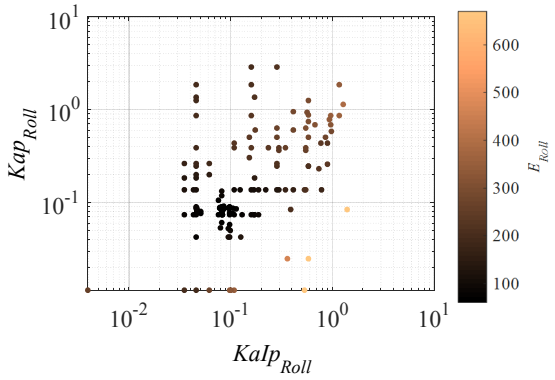

Fig. 7. Distribution of evaluation value on design space.

Figure 8 shows the transition of the evaluation function in pull-up phase optimization. It indicates that the optimization was sufficiently converged. Figure 9 shows the distribution of the evaluation value on the design space. The optimal combination of the aileron and rudder gains were obtained as [$Kap_{Pull\ nom}$, $KaIp_{Pull\ nom}$, $Krr_{Pull\ nom}$, $KrIr_{Pull\ nom}$] = [0.0590, 0.1357, -0.0131, -0.0032].

Finally, the Monte-Carlo simulation was performed to confirm the control performance of the obtained gains. 136 dispersions including 12 basic dispersions in Table 3 were changed randomly in each simulation. A number of the simulations were 2001. Here, a confidence interval of the obtained success rate was about ±1% with a significance level of 5%.[10] Figure 10 shows the histogram of the absolute difference between the desired heading and the airplane heading at the end of the pull-up phase. All results of the difference were within 60 degrees and satisfied the given requirement. It is clear that the robust control gains were found by the proposed method. Even though the quality of the solution might be same or less than the solution using a high-cost method, the proposed method was able to obtain practically sufficient solution as shown in Fig. 10.

7. Conclusion

The robust control gains for the Mars Airplane Balloon Experiment-1 was automatically and efficiently determined through optimization using evolutionary computing technique. Each combination of the control gains were evaluated through the calculations for a finite number of the principal fluctuation conditions. The robustness of the solution of this method was ensured because the highly sensitive dispersion parameters were extracted for the principal fluctuation conditions. The sufficiently robust solution was obtained with lower

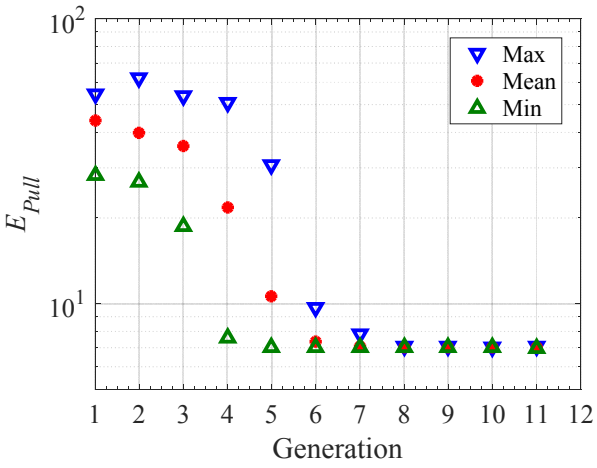

Fig. 8. Transition of evaluation function in pull-up phase optimization.

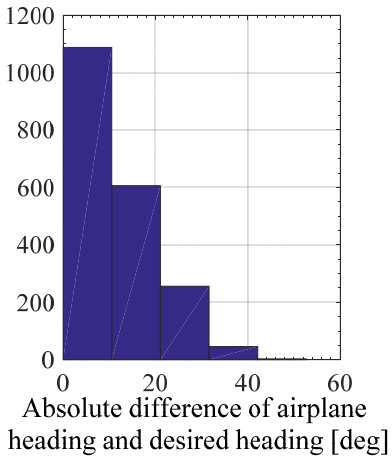

Fig. 10. Histogram of absolute difference of the airplane heading and desired heading at the end of the pull-up phase.

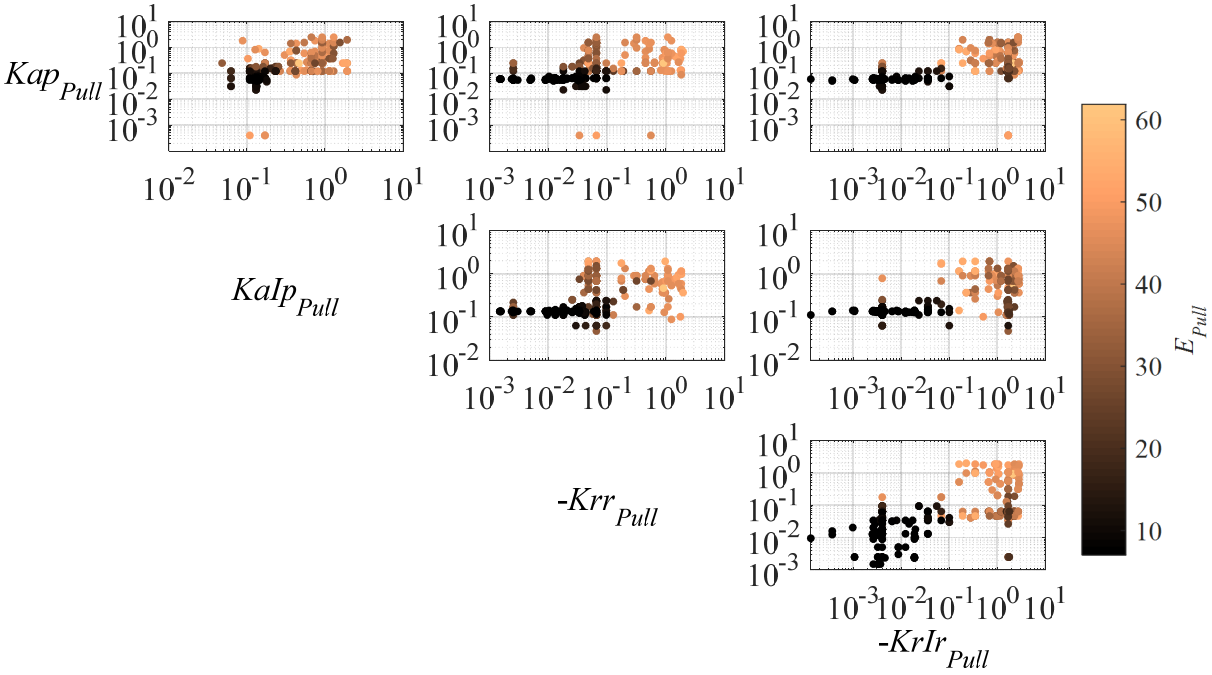

Fig. 9. Distribution of evaluation value on design space.

calculation cost than the method using Monte-Carlo simulation. Obtained control gains were used in MABE-1 and performed well. Also, this method contributed to reduce the amount of the development time.

Acknowledgments

In conducting this flight test, we received a strategic development research grant from the advisory committee for space engineering, Institute of Space and Astronautical Science (ISAS), the Japan Aerospace Exploration Agency (JAXA). We used the balloon flight opportunity provided by ISAS, JAXA. We are also supported by the scientific ballooning research and operation group of ISAS, JAXA.

References

1) Nagai, H. and Oyama, A.: Development of Japanese Mars Airplane, Proceedings of the 67th International Astronautical Congress, IAC-16-A3.3A.5x35104, Guadalajara, Mexico, Sep. 2016.
2) Oyama, A., Nagai, H., Tokutake, H., Fujita, K., Anyoji, M., Toyota, H., Miyazawa, Y., Yonemoto, K., Okamoto, M., Nonomura, T., Motoda, T., Takeuchi, S., Kamata, Y., Otsuki, M., Asai, K., and Fujii, K.: Flight System of Mars Airplane Balloon Experiment-1 (MABE-1), Proceedings of the 31st International Symposium on Space Technology and Science, 2017-k-42, June. 3-9, 2017.
3) Oyama, A., Nagai, H., Tokutake, H., Fujita, K., Anyoji, M., Toyota, H., Miyazawa, Y., Yonemoto, K., Okamoto, M., Nonomura, T., Motoda, T., Takeuchi, S., Kamata, Y., Otsuki, M., Asai, K., and Fujii, K.: Aerodynamic Data Acquisition of Mars Airplane by High Altitude Flight Test, *JAXA Research and Development Report Research, Reports on High Altitude Balloons*, JAXA-RR-16-008, 2017 (in Japanese).
4) Porter, B. and Jones, A. H.: Genetic Tuning of Digital PID Controllers, *Electronics Letter*, **28** (1992), 843/844 10.
5) Krishnakumar, K. and Goldberg, D. E.: Control System Optimization Using Genetic Algorithm, *J. Guidance, Control, and Dynamics*, **15** (1992), pp.735-740.
6) Ghazi, G. and Botez, R. M.: New Robust Control Analysis Methodology for Lynx helicopter and Cessna Citation X Aircraft Using Guardian Maps, Genetic Algorithms and LQR Theories Combinations, Proceedings of the AHS 70th Annual Forum, Montreal, Quebec, Canada, May 20–22, 2014.
7) Avanzini, G. and Minisci, E. A.: Evolutionary Design of a Full-envelope Flight Control System for an Unstable Fighter Aircraft, Proceedings of the IEEE Congress on Evolutionary Computation (CEC), 2010.
8) Motoda, T., Stengel, R. F., and Miyazawa, Y.: Robust Control System Design Using Simulated Annealing, *J. Guidance, Control, and Dynamics*, **25** (2002), pp.267-274.
9) Anyoji, M., Okamoto, M., Hidaka, H., Nonomura, T., Oyama, A. Kozo Fujii, K.: Planetary Atmosphere Wind Tunnel Tests on Aerodynamic Characteristics of a Mars Airplane Scale Model, *Trans. JSASS, Aerospace Technology Japan*, **12**, ists29 (2014), pp. Pk_7-Pk_12.
10) Okamoto, M.: *Probability and Statistics for Engineers*, Corona publishing, Tokyo, 2013 (in Japanese).